SAND98-1874C

CHEMICAL KINETICS FOR MODELING SILICON EPITAXY FROM CHLOROSILANES

Pauline Ho
Sandia National Laboratories
Albuquerque, NM 87185-0601

Ajit Balakrishna, Juan M. Chacin, Annalena Thilderkvist,
Brian Haas, and Paul B. Comita
Applied Materials
Santa Clara, CA 95054

A reaction mechanism has been developed that describes the gas-phase and surface reactions involved in the chemical vapor deposition of Si from chlorosilanes. Good agreement with deposition rate data from a single wafer reactor with no wafer rotation has been attained over a range of gas mixtures, total flow rates, and reactor temperatures.

INTRODUCTION

The use of numerical models of Chemical Vapor Deposition (CVD) systems promises to facilitate equipment design and process optimization, but such models require a fairly complete description of the chemistry occurring in the system to be broadly applicable. The CVD of silicon from chlorosilanes is widely used to deposit epitaxial films in the semiconductor industry. It is a good candidate for numerical simulations because there is a reasonable amount of kinetic and thermochemical information on chlorosilanes available in the physical chemistry literature. These include studies of both gas-phase and surface reactions, although uncertainties remain high for the latter. Drawing on this literature, we have developed a chemical reaction mechanism to describe CVD from trichlorosilane. Simulations using this mechanism agree well with experimental deposition rates measured along the centerline of an Applied Materials Epi Centura single-wafer reactor (no wafer rotation) over a range of gas mixtures, total flow rates, and temperatures.

In this work, we primarily used software from the CHEMKIN Collection (1) for describing reacting flow systems. AURORA, a 0-D simulator, provides information on reaction rates-of-progress and sensitivity analysis that is valuable in developing a mechanism. CRESLAF, a 2-D boundary-layer flow code, was used to simulate the flow in a the reactor as flow between two plates, with guidance from 3-D simulations of the heat and mass transport using CFD-ACE (2). This work does not include all the effects of the complex flows, but in the future, we expect to couple the chemistry described here with 3-D flow simulations.

REACTION MECHANISM

The gas-phase reactions included in the mechanism are shown in Table I. The rate parameters for reactions G1 and G2, the decomposition of tri- and dichlorosilane to $SiCl_2$, are taken from the experimental measurements by Walker, et al. (3) For G3, the decomposition of $SiCl_2H_2$ to HSiCl and HCl, the rate parameters are from the quantum chemical calculations of Su and Schlegel (4). The remaining gas-phase reactions, G4-G9, involve chlorinated disilanes and are from the quantum-chemistry calculations and kinetic modeling by Swihart and Carr (5). These disilane species never attain significant concentrations and could have been eliminated to reduce the size of the mechanism. The pressure-dependence of the unimolecular reactions is not explicitly included, as the reactor of interest is operated at atmospheric total pressure where the rates should be close to the high-pressure limits. All the reactions in the gas are reversible, with thermochemical parameters obtained from quantum chemistry calculations (6).

The surface reactions in our mechanism are given in Table II. We use pairs of irreversible reactions rather than reversible reactions because: 1) the literature may contain information on either the forward or backward reaction, or both; and 2) this avoids the need to include thermochemical data for surface species, which are not generally available. The pairs of reactions were checked to ensure that they correspond to reasonable enthalpies and entropies of reaction. We define three surface species: an open silicon site Si(s), a H bonded to a surface silicon SiH(s) and a Cl bonded to a surface silicon SiCl(s). Although more complex surface species such as $SiCl_3$(s) are known, we assume that they decompose to the simple species under the high-temperature conditions of interest. We use a site density of 1.162×10^{-9} moles cm^{-2} for the Si(100) surface based on the bulk density of Si (2.33 g cm^{-3}). Si(B) represents a Si atom in the bulk.

Reactions S1-S3 are the dissociative adsorption of trichlorosilane, dichlorosilane, and tetrachlorosilane on open surface silicon sites. George and coworkers (7) reported that $SiCl_2H_2$ undergoes precursor-mediated adsorption, followed by step-wise dissociation. We combine these steps into a single net reaction, and use the slightly negative activation

Table I. Gas-Phase Reactions

No.	Reaction	A (s^{-1})	E_a (cal/mole)	Source
G1	$SiCl_3H \leftrightarrow HCl + SiCl_2$	3.162×10^{14}	72900.	Ref. 3
G2	$SiCl_2H_2 \leftrightarrow SiCl_2 + H_2$	3.162×10^{13}	69300.	Ref. 3
G3	$SiCl_2H_2 \leftrightarrow HSiCl + HCl$	6.918×10^{14}	75800.	Ref. 4
G4	$H_2ClSiSiCl_3 \leftrightarrow SiCl_4 + SiH_2$	1.585×10^{13}	55500.	Ref. 5
G5	$H_2ClSiSiCl_3 \leftrightarrow SiCl_3H + HSiCl$	3.162×10^{13}	49800.	Ref. 5
G6	$H_2ClSiSiCl_3 \leftrightarrow SiCl_2H_2 + SiCl_2$	6.310×10^{13}	44300.	Ref. 5
G7	$Si_2Cl_5H \leftrightarrow SiCl_4 + HSiCl$	5.012×10^{13}	52300.	Ref. 5
G8	$Si_2Cl_5H \leftrightarrow SiCl_3H + SiCl_2$	7.943×10^{13}	45900.	Ref. 5
G9	$Si_2Cl_6 \leftrightarrow SiCl_4 + SiCl_2$	1.585×10^{14}	48800.	Ref. 5

DISCLAIMER

Table II. Surface Reactions

No.	Reaction	A (in cm, s, mole)	E_a (cal/mole)	Comments
S1	$SiCl_3H + 4Si(S) \rightarrow Si(B) + SiH(S) + 3SiCl(S)$	4.1×10^{-4}	-3800.0	S[a], 1st [b], Refs. 7 and 9
S2	$SiCl_2H_2 + 4Si(S) \rightarrow Si(B) + 2SiH(S) + 2SiCl(S)$	1.20×10^{-3}	-3800.0	S[a], 1st [b], Refs. 7 and 8
S3	$SiCl_4 + 4Si(S) \rightarrow Si(B) + 4SiCl(S)$	3.0×10^{-5}	-3800.0	S[a], 1st [b]
S4	$SiCl_2 + 2Si(S) \rightarrow Si(B) + 2SiCl(S)$	2.2	15000.0	S[a], fit
S5	$2SiCl(S) + Si(B) \rightarrow SiCl_2 + 2Si(S)$	4.758×10^{22}	67000.0	Ref. 7
S6	$H_2 + 2Si(S) \rightarrow 2SiH(S)$	0.1	17300.0	S[a], 1st [b], Ref. 11
S7	$2SiH(S) \rightarrow 2Si(S) + H_2$	8.606×10^{23}	57100.0	1st [b]
S8	$HCl + 2Si(S) \rightarrow SiH(S) + SiCl(S)$	0.07	5000.0	S[a], fit to DR data
S9	$SiH(S) + SiCl(S) \rightarrow 2Si(S) + HCl$	4.0×10^{25}	71500.0	Refs. 7 and 10
S10	$HSiCl + 2Si(S) \rightarrow Si(B) + SiH(S) + SiCl(S)$	0.06	5000.0	S[a], fit

a indicates that the rate coefficient is a sticking coefficient for the gas-phase species.

b indicates that the coverage-dependence capabilities of Surface CHEMKIN have been used to make the reaction first-order in the relevant surface species.

energy reported in this $SiCl_2H_2$ study for all three. Although this approach makes these surface reactions formally fourth order in the surface species, we modified the rate expression by the surface coverage to make them first order in Si(s). The pre-exponential factors for reaction S2 was obtained from a combination of the work by George and coworkers (7) and fits to some molecular-beam measurements of $SiCl_2H_2$ reactive sticking coefficients (8). The A factor for reaction S1 was obtained by fitting a sticking coefficient at a single temperature reported by Dillon, et al., (9), while the A factor for reaction S3 was assumed to be proportionately lower than values for S1 and S2. The rate parameters for reaction S5, $SiCl_2$ desorption, were taken from Ref. 7. For S9, HCl desorption, we use values intermediate between those from that paper and those reported by Mendicino and Seebauer (10). For reactions S4 and S10, we used activation energies from analogous gas-phase silylene insertion reactions, and adjusted the A factors to give reasonable sticking coefficients that helped fit the deposition rate data. For S6, the dissociative adsorption of H_2, we use the rate parameters reported by Bratu, et al. (11), while its reverse, S7 is based on previous silane work. The rate parameters for S8, the dissociative adsorption of HCl, were obtained by fitting the deposition rate data.

RESULTS

Figures 1-3 show comparisons between experimental centerline deposition rate data in an Applied Materials Epi Centura reactor and the numerical simulations as a function of substrate temperature, gas mixture, and total flow rate. The base conditions for these experiments are: an input mixture of 0.0438 (mole fraction) $SiCl_3H$ in H_2, atmospheric

total pressure, 1100°C, total flow rate 60 slm, and no wafer rotation. Overall, the agreement between model and experiment is excellent. As expected, there are some discrepancies at the beginning of the wafer, where the boundary-layer simulations oversimplifies the gas velocities and temperatures in the entrance region.

Figure 4 shows contours from the 2-D simulations of the gas temperature, $SiCl_3H$, HCl and $SiCl_2$ mole fractions as a function of position above and along the hot substrate. The heating of the gas, as well as the depletion of the $SiCl_3H$ and the build-up of HCl and $SiCl_2$ near the hot surface can be seen easily. The gradients shown here demonstrate the expected importance of transport limitations in this system. Analyzing the rates-of-progress and reaction sensitivity information from the 0-D simulations, as well as the mass-fluxes to the surface in the 2-D simulations also gives the following results. The Si deposition rate appears to be most sensitive to the rates of H_2 and HCl adsorption / desorption, and less sensitive to the rates of $SiCl_2$ adsorption / desorption. The deposition rate is insensitive to the rate of $SiCl_3H$ adsorption except at the lower temperatures, even though this species is responsible for most of the mass flux to the surface.

ACKNOWLEDGMENTS

The work at Sandia was partially supported under CRADA No. 1251 with Applied Materials, and partially for the Office of Basic Energy Sciences. Sandia is a multiprogram laboratory operated by Sandia Corporation, a Lockheed Martin Company, for the United States Department of Energy under Contract DE-AC04-94AL85000.

REFERENCES

1. R. J. Kee, F. M. Rupley, J. A. Miller, M. E. Coltrin, J. F. Grcar, E. Meeks, H. K. Moffat, A. E. Lutz, G. Dixon-Lewis, M. D. Smooke, J. Warnatz, G. H. Evans, R. S. Larson, R. E. Mitchell, L. R. Petzold, W. C. Reynolds, M. Caracotsios, W. E. Stewart, and P. Glarborg , Chemkin Collection , vers. 3.02 , Reaction Design, Inc., (1997).
2. CFD Research Corporation, Huntsville, Alabama.
3. K. L. Walker, R. E. Jardine, M. A. Ring, H. E. O'Neal, Int. J. Chem. Kinet., *30*, 69 (1998).
4. M.-D. Su and H. B. Schlegel, J. Phys. Chem., *97*, 9981 (1993).
5. M. T. Swihart and R. W. Carr, J. Phys. Chem., *A102*, 1542 (1998).
6. P. Ho, M. E. Coltrin, J. S. Binkley, and C. F. Melius, J. Phys. Chem. *89*, 4647 (1985); P. Ho and C. F. Melius, J. Phys. Chem. *94*, 5120 (1990); M. D. Allendorf and C. F. Melius, J. Phys. Chem. *97*, 720 (1993).
7. P. A. Coon, M. L. Wise, and S. M. George, J. Crystal Growth, *130,* 162 (1993).
8. R. J. Buss and P. Ho, unpublished.
9. A. C. Dillon, M. L. Wise, M. B. Robinson, and S. M. George, J. Vac. Sci. Technol., *A13*, 1 (1995).
10. M. A. Mendicino and E. G. Seebauer, J. Electrochem. Soc., *140*, 1786 (1993).
11. P. Bratu, K. L. Kompa, U. Höfer, Chem. Phys. Lett., *251*, 1 (1996).

FIGURES

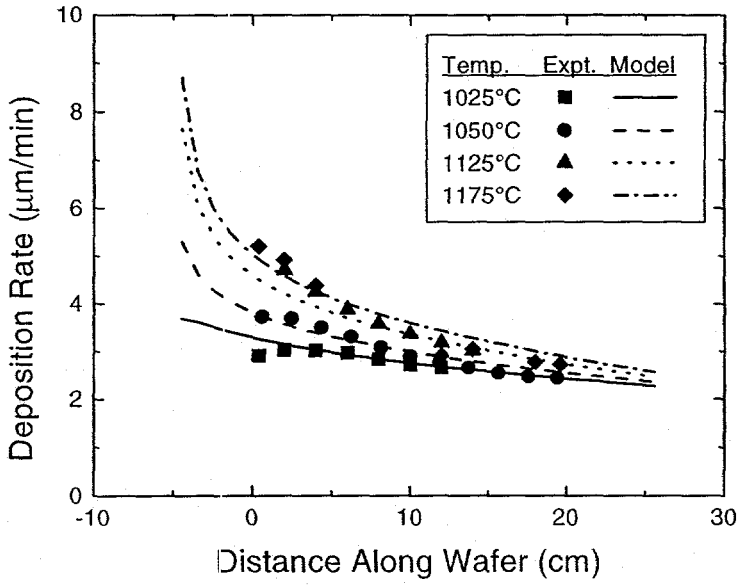

Figure 1. Comparison between model predictions and experimental deposition rates as a function of position in the reactor for four different substrate temperatures.

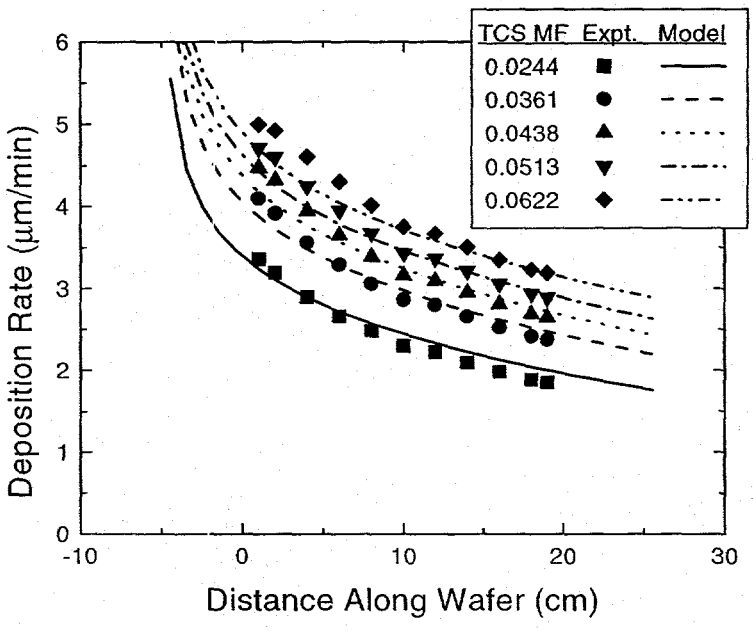

Figure 2. Comparison between model predictions and experimental deposition rates as a function of position in the reactor for five different $HSiCl_3/H_2$ gas mixtures.

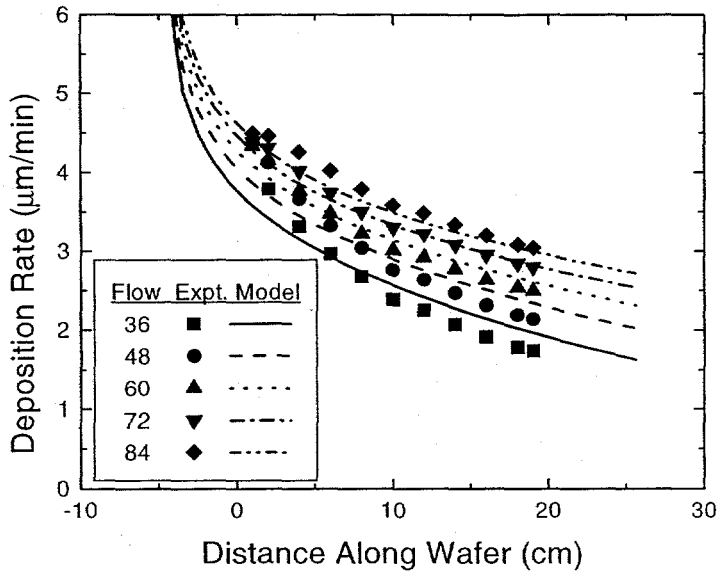

Figure 3. Comparison between model predictions and experimental deposition rates as a function of position in the reactor for four different total flow rates.

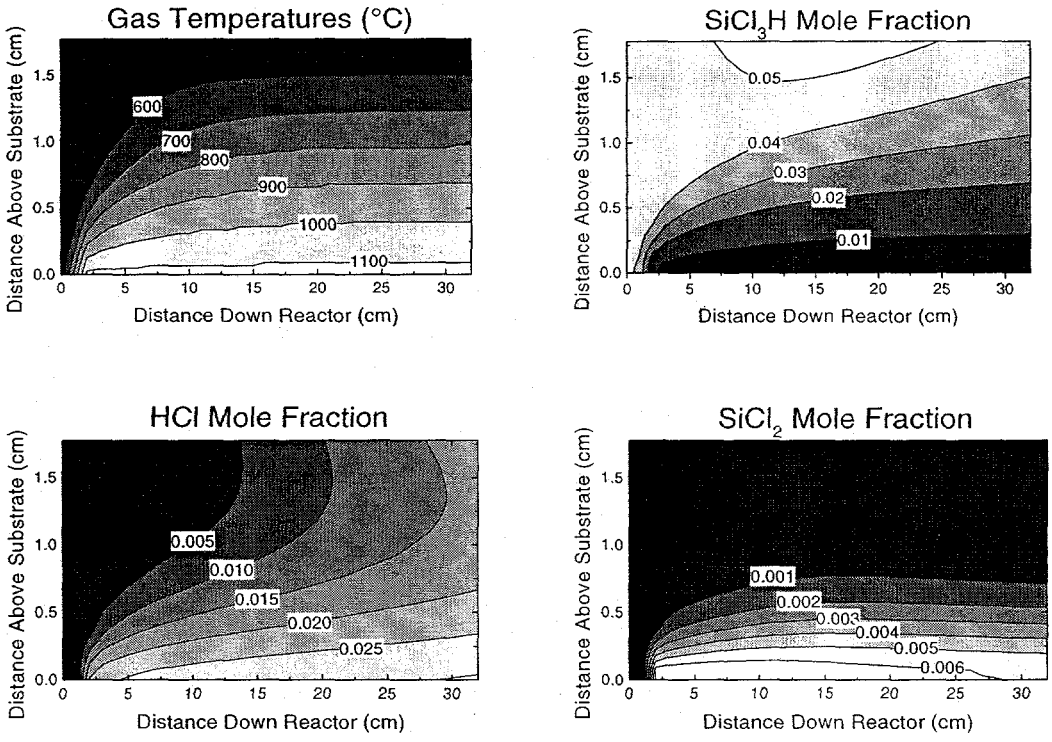

Figure 4. Temperature and species contours from CRESLAF simulations.